Emergent Collective Phenomena in a Mixture of Hard Shapes through Active Rotation

Nguyen H. P. Nguyen,[1] Daphne Klotsa,[2] Michael Engel,[2] and Sharon C. Glotzer[2,3,*]
[1]Department of Mechanical Engineering, University of Michigan, Ann Arbor, Michigan 48109, USA
[2]Department of Chemical Engineering, University of Michigan, Ann Arbor, Michigan 48109, USA
[3]Department of Materials Science and Engineering, University of Michigan, Ann Arbor, Michigan 48109, USA
(Received 9 August 2013; revised manuscript received 4 October 2013; published 20 February 2014)

We investigate collective phenomena with rotationally driven spinners of concave shape. Each spinner experiences a constant internal torque in either a clockwise or counterclockwise direction. Although the spinners are modeled as hard, otherwise noninteracting rigid bodies, their active motion induces an effective interaction that favors rotation in the same direction. With increasing density and activity, phase separation occurs via spinodal decomposition, as well as self-organization into rotating crystals. We observe the emergence of cooperative, superdiffusive motion along interfaces, which can transport inactive test particles. Our results demonstrate novel phase behavior of actively rotated particles that is not possible with linear propulsion or in nondriven, equilibrium systems of identical hard particles.

DOI: 10.1103/PhysRevLett.112.075701 PACS numbers: 64.75.Xc, 47.11.Mn, 89.75.Kd

Introduction.—Active matter is a rapidly growing branch of nonequilibrium soft matter physics with relevance to biology, energy, and complex systems [1]. In active matter, dissipative, steady-state structures far from equilibrium can emerge in systems of particles by converting energy to particle motility [1,2]. Recent works reported novel collective behavior such as giant number fluctuations [3], clustering [4], swarming [5], fluid-solid phase separation of repulsive disks [6,7], and collective rotors [8]. Effective interactions emerging between hard, self-propelled particles were shown to cause phase separation and coexistence [6,9–12]. Experimentally, some of these phenomena were demonstrated by driving the system via vibration [13], chemical reaction [14], diffusiophoresis [12], and light activated propulsion [15]. To date, most studies have focused on self-propulsion where the constant input of energy to each particle goes directly into translational motion and, hence, active forces couple to particle velocities. Converting the input of energy into rotational motion, however, does not directly influence translational motility, and couples only to the particles' angular momentum. We denote such a coupling of active driving forces to angular velocity as active rotation.

Active rotation may be achieved by various methods, e.g., external magnetic fields [16,17] and optical tweezers [18,19]. Biological organisms, such as dancing algae [20] and clusters of sperm cells [21], can spin naturally. Certain self-propelled anisotropic shapes exhibit circular motion [8,22]. Rotating particles submersed in a fluid experience hydrodynamic interactions that can be attractive or repulsive through the formation of vortices [16,23]. Collective phenomena involve synchronization and self-proliferating waves [24], and vortex arrays [25]. Beyond these examples, however, the potential use of active rotation for pattern formation and self-organization in driven systems is only starting to be investigated systematically. In this Letter, we show with computer simulations that effective interactions emerge between spinners rotating in the same direction, and between oppositely rotating spinners, due to the active motion itself. The result is phase separation, rotating crystals, cooperative and heterogeneous dynamics leading to superdiffusive motion, and complex phase behavior.

Model and methods.—Our spinner particle is modeled by four peripheral disks of radius σ rigidly attached to a central disk of radius 3σ at each of the compass points, Fig. 1(a). The system is governed by a set of coupled Langevin equations for translation and rotation

$$M\frac{\partial \boldsymbol{v}_i}{\partial t} = \boldsymbol{F}_i - \gamma_t \boldsymbol{v}_i + \boldsymbol{F}_i^R, \tag{1}$$

$$I\frac{\partial \omega_i}{\partial t} = \tau_i^D + \tau_i - \gamma_r \omega_i + \tau_i^R, \tag{2}$$

where M, I, $\boldsymbol{v}_i$, and ω_i are mass, moment of inertia, and translational and angular velocity. Each spinner is driven by an external torque $\tau_i^D = \pm\tau^D$ of constant magnitude, with positive sign for clockwise spinners ("A") and negative sign for counterclockwise spinners ("B"). Spinners are hard particles that interact via a purely repulsive contact potential, resulting in internal forces $\boldsymbol{F}_i$ and torques τ_i. Energy is dissipated through translational and rotational drag coefficients γ_t and γ_r. Noise is included via Gaussian random forces $\boldsymbol{F}_i^R = \sqrt{2\gamma_t kT_0}R(t)$ and torques $\tau_i^R = \sqrt{2\gamma_r kT_0}R(t)$ [27] that model a heat bath at temperature T_0. Random forces are applied directly to the centroid of each spinner.

Langevin dynamics simulations are performed on graphic processing units (GPUs) with the HOOMD-blue software package [28] using up to 16 384 spinners, half of which are driven to always spin clockwise, and the rest

driven to spin counterclockwise. Each disk is treated as a point mass m located at the center, which means $M = 5m$ and $I = 64m\sigma^2$. The hard contact is modeled via a WCA potential with parameter ϵ [29] shifted to the surface of the spinner such that its range is a small fraction of the particle diameter, thereby approximating hard shapes. In the low Reynolds number limit, the translational and rotational drag coefficients are related through the Stokes-Einstein and Stokes-Einstein-Debye relations. If we approximate the spinner as a disk of effective radius $\tilde{\sigma}$, the relations for disks give $\gamma_r = \frac{4}{3}\tilde{\sigma}^2\,\gamma_t = 100\sigma^2\gamma_t$. We choose σ and ϵ as the units of length and energy. The unit of time is $t_0 = \sqrt{m\sigma^2/\epsilon}$. Thermal noise is specified by $T^* = kT_0/\epsilon$. Throughout the Letter, we report results for $\tau^D/\epsilon = 1$ and $\gamma_t/(t_0^{-1}m) = 1$ unless stated otherwise.

Nonequilibrium phase behavior.—Following equilibration with active rotation turned off, the time evolution of the active system is characterized by an approach towards steady state. Energy input to rotational motion by the applied torque is transferred to the translational degrees of freedom and then dissipated by drag forces. In steady state, we observe that the energy balance $\kappa = E_{\text{trans}}/E_{\text{total}}$ between translational and total kinetic energy converges. While the nondriven 2D system has $\kappa = 2/3$ as dictated by the equipartition theorem, a value $\kappa < 2/3$ quantifies the nonequilibrium character.

We analyze the behavior of κ as a function of density ϕ and noise T^*. As shown in Fig. 1(b), at low density the driven rotational motion dominates translational motion and $\kappa \to 0$. With increasing density, the number of collisions increases and κ approaches the equipartition value. Interestingly, we find a nonequilibrium phase transition in the range $0.25 < \phi_c < 0.48$. For zero noise, the increase in κ is sharp, and possibly discontinuous, but becomes continuous as the noise increases. Based on the observation of a rapidly increasing length scale in the pair distribution function $g_{\text{AB}}(r)$ of opposite spinners, we identify this transition as the phase separation of the system into A-rich and B-rich domains. Increasing the noise from zero at fixed values of applied torque [inset of Fig. 1(b)] initially lowers the critical density ϕ_c, because particle collisions that facilitate the onset of phase separation are more frequent. If the system is too noisy, phase separation is hindered and the trend is reversed.

For the remainder of the Letter, we follow Refs. [8,25,30] and neglect the role of noise by setting $T^* = 0$. In this limit, the dynamics of the system is characterized by two parameters, the density ϕ and the low-density dimensionless steady-state angular velocity $\omega_0 = \tau^D t_0/\gamma_r$, which is a measure of activity. Figure 1(c) shows the ϕ-ω_0 nonequilibrium phase diagram at (or near) steady state. Movies of the spinner dynamics can be found in the Supplemental Material [26].

At low densities, we find a frozen (absorbing [31] or dilute [25]) state, where the spinners are fixed in place and

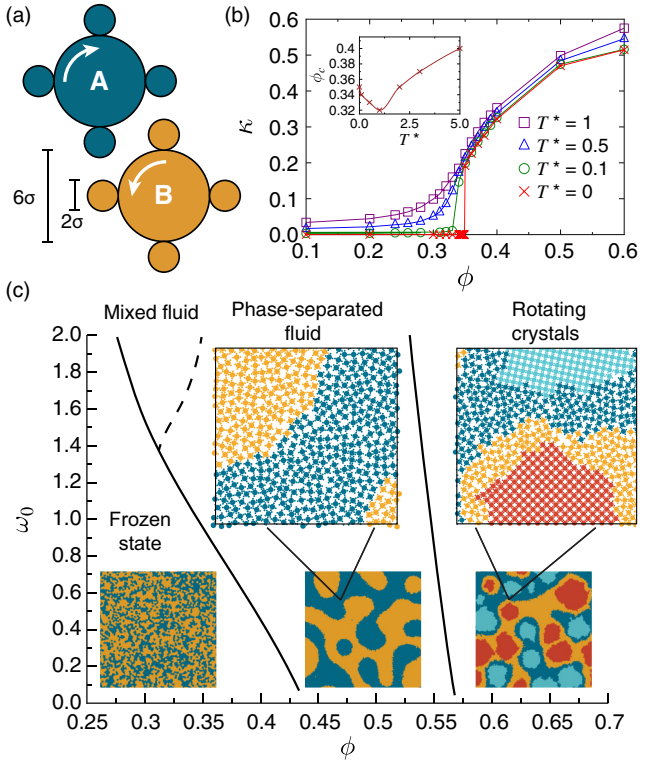

FIG. 1 (color online). (a) Clockwise (A) and counterclockwise (B) spinners. (b) The ratio of translational to total kinetic energy κ indicates the presence of a phase transition ($\omega_0 = 1$). Error bars are smaller than the symbols. The inset shows the critical density ϕ_c as a function of noise T^*. (c) Nonequilibrium phase diagram based on simulation data (see the Supplemental Material [26]) at $T^* = 0$. Lines indicate phase boundaries. Insets show representative snapshots as the system approaches steady state. A and B spinners in the fluid (crystal) phase are shown in dark (light) blue and orange (red) colors. Fifty:fifty mixtures are used in (b),(c).

rotate at angular velocity ω_0. Translational motion does not couple to rotation, the system is nonergodic, and drag forces dominate. The few collisions that occur from the initial kinetic energy (random initialization) die out quickly due to dissipation [32].

At higher density, the frequency of collisions increases. When the time interval between collisions is sufficiently short, i.e., comparable to the characteristic time m/γ_t for energy dissipation, nonstop chained collisions can sustain the transfer from rotational to translational energy. Depending on ω_0, we observe a transition to either a mixed fluid or a phase separated fluid. While spinners with high activity, $\omega_0 \geq 1.2$, display two transitions (first to the mixed fluid, then phase separation), these transitions merge for lower ω_0.

As the density increases further, the spinners organize into crystals that rotate collectively about their centers of mass; particles no longer rotate about their individual centers. The critical density decreases as the activity increases in agreement with Ref. [6], but not with Ref. [7].

If crystallization occurs before phase separation is completed, the crystal size is limited by the phase separating domains. The angular velocity of a crystal decreases with radius, similar to rotors assembled from polymers by self-propelled bacteria [33]. Dynamically, this phase represents a new kind of active crystal: a rotating crystal, distinct from the two previously reported types, traveling and resting crystals [34].

Effective interaction between spinners.—We measure the time evolution of the characteristic domain size. Domains coarsen over time with $t^{1/3}$ as shown in Fig. 2(a) by determining the first zero of $g_{\mathrm{AB}}(r,t)$. The peak height of the structure factor scales as $t^{2/3}$ (see the Supplemental Material [26]). Together, these behaviors are typical for spinodal decomposition of a binary mixture in 2D in the absence of hydrodynamics [35]. The domain size growth exponent is similar to that measured in a biological system of self-organizing mussels [36], but different from that found in other systems of self-propelled colloids [6,11].

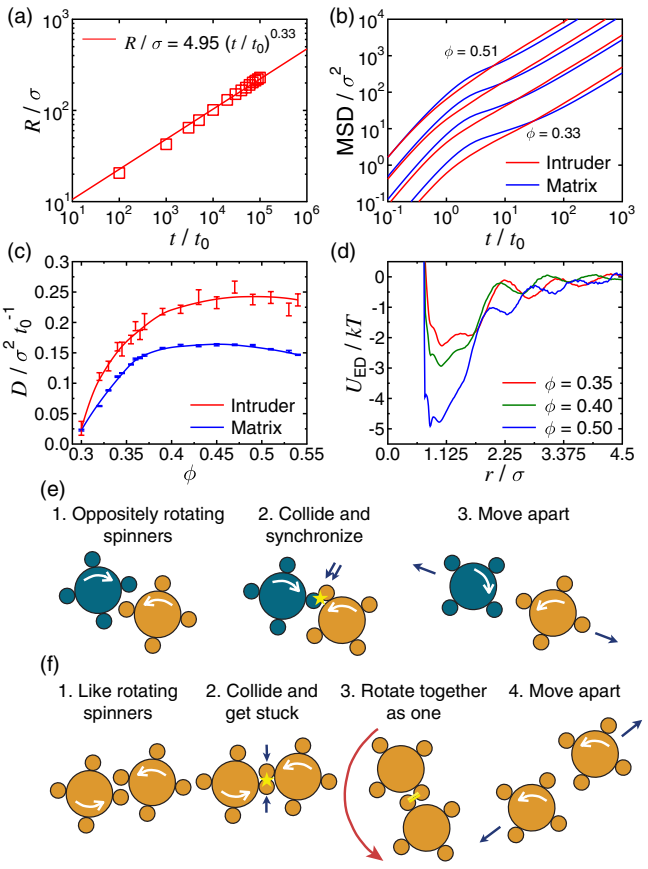

FIG. 2 (color online). (a) Domain size growth for a 50:50 mixture of spinners during phase separation ($\phi = 0.5$). (b),(c) Comparison of (b) mean-squared displacements and (c) translational diffusion coefficient D for an intruder in a matrix of opposite spinners. Curves in (b) at different densities are offset for clarity. (d) Effective demixing potential obtained for $N_A = 100$ and $N_B = 2$. In (a)–(d), activity is set to $\omega_0 = 1$. (e),(f) Typical interaction of (e) two opposite and (f) two like spinners.

The origin of the phase separation is investigated with a system of one B spinner (the intruder) in a dense matrix of A spinners. We compare their mean-squared displacements $\mathrm{MSD} = \langle |\boldsymbol{x}_i(t) - \boldsymbol{x}_i(0)|^2 \rangle$ in Fig. 2(b). While matrix particles have higher translational kinetic energy as seen in the ballistic regime $t < t_0$, the curves cross and diffusion of the intruder is faster for $t \gg t_0$. The MSD of the matrix has a plateau indicative of caging. We extract the translational diffusion coefficient D and plot it as a function of density in Fig. 2(c). With increasing density, diffusion speeds up and the gap between intruder and matrix spinners widens.

We investigate the effective interaction between N_B intruders among N_A matrix spinners by mapping our nonequilibrium system to an equilibrium system of isotropic particles interacting with pair potentials. The mapping is achieved via the effective demixing (ED) potential, which describes the preference for demixing (see the Supplemental Material [26]). The ED potential quantifies the difference in kinetic behavior between like spinners and unlike spinners in the limit of a vanishing density of intruders, $n_B = N_B/(N_A + N_B)$. It is defined as

$$U_{\mathrm{ED}}(r) = -kT \lim_{n_B \to 0} \log\left(\frac{g_{\mathrm{BB}}(r)}{g_{\mathrm{BA}}(r)}\right). \tag{3}$$

Here, g_{BB} and g_{BA} are type-specific radial distribution functions. The definition guarantees that in the absence of external torque, $U_{\mathrm{ED}}(r) = 0$. In the presence of external torque we find an attractive well in $U_{\mathrm{ED}}(r)$ of several kT [37] that deepens with increasing density, Fig. 2(d). At the critical density $\phi_c = 0.35$, the well depth is about $2kT$. This value of interaction strength is comparable to the critical attraction for the vapor-liquid transition of 2D Lennard-Jones liquids [38] and to the critical reduced interaction in the 2D Ising model, $2.269kT$ [39].

The microscopic origin of the effective interaction can be understood by comparing pairs of neighboring spinners. Consider two opposite spinners, Fig. 2(e). The "teeth" of the gearlike spinners move together for part of the cycle, synchronizing their rotation when in contact due to steric restriction, and then move apart. Now consider two spinners rotating in the same direction, Fig. 2(f). Since the tangential velocities at contact are in opposite directions, the spinners momentarily "stick" sterically. They cannot spin about their individual axes and instead transfer their angular momentum momentarily to the pair and rotate together for part of the cycle before moving apart. The consequence is a longer contact time for like spinners compared to opposite spinners, breaking the symmetry between otherwise identical particles and resulting in an emergent, effective attraction between like neighboring spinners.

Collective dynamics at interfaces and transport.—As spinners phase separate, they form interfaces separating regions of opposite rotation. The short-time diffusion

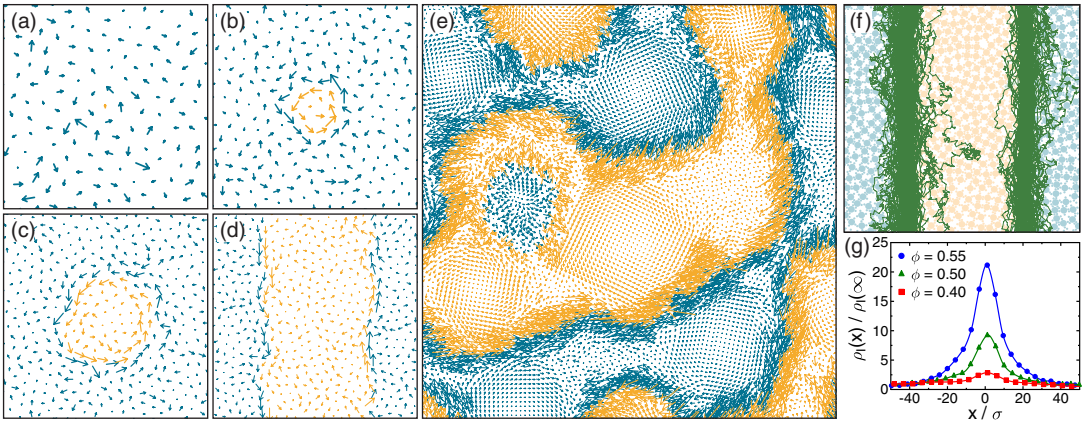

FIG. 3 (color online). (a)–(d) Vector plots show the short-time diffusion $\Delta \boldsymbol{x}(t)$ in systems of $N = 576$ spinners with different numbers of intruders: (a) one, (b) 2%, (c) 10%, and (d) 50%. (e) Large system during phase separation at a density where crystallization occurs. Observation time windows are (a)–(d) $10t_0$ and (e) $t = 100t_0$. (f) Trajectories of inactive particles (green) and (g) their probability density close to an interface. We use $\omega_0 = 1$. Densities are (a–d),(f) $\phi = 0.5$ and (e) $\phi = 0.6$.

$\Delta \boldsymbol{x}(t) = \boldsymbol{x}(t) - \boldsymbol{x}(0)$ is visualized for a density where phase separation, Figs. 3(a)–3(d), and also crystallization, Fig. 3(e), occur. We observe that the translational dynamics of the spinners is heterogeneous and cooperative, in particular at the interfaces. While diffusion is Brownian in the bulk, spinners move linearly along the interface in a superdiffusive manner with MSD $\propto t^2$. As phase separation progresses, the total length of the interfaces decreases, reducing the number of superdiffusive spinners. Interestingly, both the translational and rotational kinetic energies are uniform across the demixed fluid (see the Supplemental Material [26]). This means spinners at interfaces do not move faster, but instead move farther in a given time window. Such dynamical behavior is reminiscent of the stringlike dynamical heterogeneity in supercooled liquids and dense colloids [40].

To investigate the possibility of extracting useful work from the active motion of the spinners, we add inactive test particles to the system. An inactive particle has the same shape, size, and hard interaction as a spinner, but is not subject to a rotational driving. From their trajectories, Fig. 3(f), we observe that inactive particles diffuse to the interface and get dragged along the interface by the current of the active spinners. This observation is confirmed by the density of inactive particles as a function of the distance x to the interface, $\rho_I(x)$, relative to their bulk density $\rho_I(\infty)$, which is strongly peaked at the interface, Fig. 3(g). The preference of inactive particles to sit at the moving interface increases with density and could be utilized for collective transport at mesoscopic scales.

Discussion.—The phase separation of rotationally driven active particles is realizable in experiments provided the particles are permanently assigned a rotation direction while being free to move translationally and collide with one another. Applying torques to photosensitive spinners through optical trapping is one promising route [19] and may even be possible on the colloidal scale where the dynamics can be observed through the microscope [15,18]. In many situations, however, restricting the rotation direction is not possible. This is in particular the case for 3D systems. Our observation of an emergent attraction between like rotating particles suggests a possible alignment [24] of the rotation axes in 3D. Whether actively rotated particles can indeed synchronize spontaneously into such a nematic spinner phase (alignment of the rotation axes) remains to be seen.

We also observe phase separation, rotating crystals, and collective transport with Brownian dynamics simulations, where the inertial term is absent and the dynamics is dominated by viscous drag forces (see the Supplemental Material [26]). This means inertia is not essential for the phenomena reported here and raises interesting questions about local conservation of angular momentum. Finally, we note that the dynamics and interaction of actively rotated particles in a fluid can be influenced by hydrodynamic interactions [16,24], which are not taken into account here. We believe the tendency towards phase separation and synchronization is robust, if hydrodynamics prefers like-rotating neighbors as in Refs. [20,23]. Studying the phase behavior of externally driven or self-rotating (internally driven) spinners in a fluid environment remains an interesting open question.

This work was supported by the Non-Equilibrium Energy Research Center (NERC), an Energy Frontier Research Center funded by the U.S. DOE (DE-SC0000989). The contributions of M. E. and S. C. G. were also supported by the DOD/ASD(R&E) (N00244-09-1-0062). D. K. acknowledges FP7 Marie Curie Actions of the European Commission (PIOF-GA-2011-302490 Actsa). N. H. P. N. also acknowledges the Vietnam Education Foundation for prior support. We thank P. Chaikin, R. Larson, R. Newman, A. Osorio, and M. Spellings for helpful discussions.

*sglotzer@umich.edu

[1] M. C. Marchetti, J. F. Joanny, S. Ramaswamy, T. B. Liverpool, J. Prost, M. Rao, and R. Aditi, arXiv:1207.2929.

[2] T. Vicsek and A. Zafeiris, Phys. Rep. **517**, 71 (2012).

[3] S. Ramaswamy, R. A. Simha, and J. Toner, Europhys. Lett. **62**, 196 (2003).

[4] F. Peruani, A. Deutsch, and M. Bär, Phys. Rev. E **74**, 030904 (2006).

[5] M. R. D'Orsogna, Y. L. Chuang, A. L. Bertozzi, and L. S. Chayes, Phys. Rev. Lett. **96**, 104302 (2006); N. H. P. Nguyen, E. Jankowski, and S. C. Glotzer, Phys. Rev. E **86**, 011136 (2012).

[6] J. Bialké, T. Speck, and H. Löwen, Phys. Rev. Lett. **108**, 168301 (2012); G. S. Redner, M. F. Hagan, and A. Baskaran, Phys. Rev. Lett. **110**, 055701 (2013).

[7] Y. Fily and M. C. Marchetti, Phys. Rev. Lett. **108**, 235702 (2012).

[8] H. H. Wensink, V. Kantsler, R. E. Goldstein, and J. Dunkel, arXiv:1306.0709.

[9] J. Tailleur and M. E. Cates, Phys. Rev. Lett. **100**, 218103 (2008).

[10] M. E. Cates and J. Tailleur, Europhys. Lett. **101**, 20010 (2013).

[11] J. Stenhammar, A. Tiribocchi, R. J. Allen, D. Marenduzzo, and M. E. Cates, Phys. Rev. Lett. **111**, 145702 (2013).

[12] I. Buttinoni, J. Bialké, F. Kümmel, H. Löwen, C. Bechinger, and T. Speck, Phys. Rev. Lett. **110**, 238301 (2013).

[13] V. Narayan, S. Ramaswamy, and N. Menon, Science **317**, 105 (2007); A. Kudrolli, G. Lumay, D. Volfson, and L. S. Tsimring, Phys. Rev. Lett. **100**, 058001 (2008); K. Roeller, J. P. D. Clewett, R. M. Bowley, S. Herminghaus, and M. R. Swift, Phys. Rev. Lett. **107**, 048002 (2011).

[14] J. Palacci, C. Cottin-Bizonne, C. Ybert, and L. Bocquet, Phys. Rev. Lett. **105**, 088304 (2010); I. Theurkauff, C. Cottin-Bizonne, J. Palacci, C. Ybert, and L. Bocquet, Phys. Rev. Lett. **108**, 268303 (2012).

[15] J. Palacci, S. Sacanna, A. P. Steinberg, D. J. Pine, and P. M. Chaikin, Science **339**, 936 (2013).

[16] B. A. Grzybowski, H. A. Stone, and G. M. Whitesides, Nature (London) **405**, 1033 (2000); B. A. Grzybowski and G. M. Whitesides, Science **296**, 718 (2002).

[17] J. Yan, M. Bloom, S. C. Bae, E. Luijten, and S. Granick, Nature (London) **491**, 578 (2012).

[18] D. G. Grier, Curr. Opin. Colloid Interface Sci. **2**, 264 (1997).

[19] J. R. Moffitt, Y. R. Chemla, S. B. Smith, and C. Bustamante, Annu. Rev. Biochem. **77**, 205 (2008); A. V. Arzola, M. Šiler, O. Brzobohatý, P. Jákl, and P. Zemánek, Proc. SPIE Int. Soc. Opt. Eng. **8458**, 84582U (2012).

[20] K. Drescher, K. C. Leptos, I. Tuval, T. Ishikawa, T. J. Pedley, and R. E. Goldstein, Phys. Rev. Lett. **102**, 168101 (2009).

[21] I. H. Riedel, K. Kruse, and J. Howard, Science **309**, 300 (2005).

[22] F. Kümmel, B. ten Hagen, R. Wittkowski, I. Buttinoni, R. Eichhorn, G. Volpe, H. Löwen, and C. Bechinger, Phys. Rev. Lett. **110**, 198302 (2013).

[23] Y. Fily, A. Baskaran, and M. C. Marchetti, Soft Matter **8**, 3002 (2012).

[24] N. Uchida and R. Golestanian, Phys. Rev. Lett. **104**, 178103 (2010).

[25] A. Kaiser and H. Löwen, Phys. Rev. E **87**, 032712 (2013).

[26] See Supplemental Material at http://link.aps.org/supplemental/10.1103/PhysRevLett.112.075701 for additional methods, movies, and figures.

[27] The random forces $R(t)$ are normalized zero-mean white-noise Gaussian processes, which assure thermodynamic equilibrium in the absence of the externally applied torques.

[28] J. A. Anderson, C. D. Lorenz, and A. Travesset, J. Comput. Phys. **227**, 5342 (2008). See also the HOOMD-blue web page http://codeblue.umich.edu/hoomd-blue.

[29] J. D. Weeks, D. Chandler, and H. C. Andersen, J. Chem. Phys. **54**, 5237 (1971).

[30] K. Drescher, J. Dunkel, L. H. Cisneros, S. Ganguly, and R. E. Goldstein, Proc. Natl. Acad. Sci. U.S.A. **108**, 10940 (2011).

[31] H. Hinrichsen, Adv. Phys. **49**, 815 (2000).

[32] Our frozen state is different from those observed under oscillatory shear [41] or with self-propulsion [42], where particles retrace their trajectories.

[33] J. Schwarz-Linek, C. Valeriani, A. Cacciuto, M. E. Cates, D. Marenduzzo, A. N. Morozov, and W. C. K. Poon, Proc. Natl. Acad. Sci. U.S.A. **109**, 4052 (2012).

[34] A. M. Menzel and H. Löwen, Phys. Rev. Lett. **110**, 055702 (2013).

[35] I. M. Lifshitz and V. V. Slyozov, J. Phys. Chem. Solids **19**, 35 (1961); S. W. Koch, R. C. Desai, and F. F. Abraham, Phys. Rev. A **27**, 2152 (1983); E. Velasco and S. Toxvaerd, Phys. Rev. Lett. **71**, 388 (1993); S. C. Glotzer, E. A. Di Marzio, and M. Muthukumar, Phys. Rev. Lett. **74**, 2034 (1995).

[36] Q.-X. Liu, A. Doelman, V. Rottschafer, M. de Jager, P. M. J. Herman, M. Rietkerk, and J. van de Koppel, Proc. Natl. Acad. Sci. U.S.A. **110**, 11905 (2013).

[37] The temperature T appearing in the ED potential is not related to the noise T^*.

[38] B. Smit and D. Frenkel, J. Chem. Phys. **94**, 5663 (1991).

[39] L. Onsager, Phys. Rev. **65**, 117 (1944).

[40] W. Kob, C. Donati, S. J. Plimpton, P. H. Poole, and S. C. Glotzer, Phys. Rev. Lett. **79**, 2827 (1997); C. Donati, J. F. Douglas, W. Kob, S. J. Plimpton, P. H. Poole, and S. C. Glotzer, Phys. Rev. Lett. **80**, 2338 (1998).

[41] L. Corté, P. M. Chaikin, J. P. Gollub, and D. J. Pine, Nat. Phys. **4**, 420 (2008).

[42] V. Schaller, C. A. Weber, B. Hammerich, E. Frey, and A. R. Bausch, Proc. Natl. Acad. Sci. U.S.A. **108**, 19183 (2011).